Electric field induced switching of poly(ethylene glycol) terminated self-assembled monolayers: A parallel molecular dynamics simulation

Satyavani Vemparala, Rajiv K. Kalia, Aiichiro Nakano, and Priya Vashishta
Collaboratory for Advanced Computing and Simulations, Department of Materials Science & Engineering, Department of Computer Science, Department of Physics & Astronomy and Department of Biomedical Engineering, University of Southern California, Los Angeles, California 90089-0242

(Received 14 October 2003; accepted 17 June 2004)

Effects of electric field on the structure of poly(ethylene glycol) (PEG) terminated alkanethiol self-assembled monolayer (SAM) on gold have been studied using parallel molecular dynamics method. An applied electric field triggers a conformational transition from all-*trans* to a mostly *gauche* conformation. The polarity of the electric field has a significant effect on the surface structure of PEG leading to a profound effect on the hydrophilicity of the surface. The electric field applied antiparallel to the surface normal causes a reversible transition to an ordered state in which the oxygen atoms are exposed. On the other hand, an electric field applied in a direction parallel to the surface normal introduces considerable disorder in the system and the oxygen atoms are buried inside. The parallel field affects the overall tilt structure of SAMs more adversely than the antiparallel field. © *2004 American Institute of Physics.* [DOI: 10.1063/1.1781120]

I. INTRODUCTION

Protein resistant surfaces play a significant role in biotechnology to stabilize cells[1–3] and to prevent the degeneration of the bulk properties of materials upon protein adsorption.[4] Recently poly(ethylene glycol) (PEG) terminated self-assembled monolayers (SAM) have attracted much attention because of their successful ability to resist protein adsorption.[5–8] This surface property is attributed to a large extent to its unique structure, i.e., helical nature[9] and number of exposed oxygen atoms. The surface structure and consequently the surface properties are highly sensitive to external parameters such as temperature,[6] electric fields,[7] and types of solvent[10] and substrate.[11]

Among these parameters, externally applied electric field is technologically most important due to its control over surface properties. Lahann and co-workers have recently demonstrated reversible switching of hydrophilicity in SAMs by the application of an electric field.[7] To optimize surface properties, it is important to atomistically understand the dependence of surface structures on applied electric field. Unfortunately the effect of electric fields on the structure of SAMs at the atomic level is not well known. Atomistic simulations based on molecular dynamics (MD) technique are expected to provide some insight into the behavior of the system.

In this paper, we study the effect of external electric fields on the atomistic structure of PEG terminated SAMs using molecular dynamics simulations on parallel computers. The paper is organized as follows. In Sec. II we describe the force field used for simulations of PEG terminated SAMs, initial setup of the system, and the schedule of the simulation. Section III describes the results of the simulations including the effect of electric field on the *gauche* conformations in PEG, the number of oxygen atoms exposed on the surface, and on the tilt structure of the system. Section IV contains the conclusions of this study.

II. METHODOLOGY

A. Interatomic potential model

In MD simulations the physical system is represented by a set of N atoms. We follow the trajectory, i.e., positions and velocities of all the atoms by numerically integrating the Newton's equations of motion.

We use the interatomic potential model in which the conformational energy (V) of a molecular system is split into bonded, nonbonded, surface interaction, and external electric field terms:

$$V = V_{\text{bonded}} + V_{\text{nonbonded}} + V_{\text{surface}} + V_{\text{electric}}. \tag{1}$$

Here V_{bonded} represents the bonded interactions that arise from bond stretching, bending, and torsions:

$$V_{\text{bonded}} = \sum_{ij} \frac{1}{2} k^s_{ij} (r_{ij} - r^0_{ij})^2 + \sum_{ijk} \frac{1}{2} k^b_{ijk} (\alpha_{ijk} - \alpha^0_{ijk})^2 + \sum_{ijkl} \frac{1}{2} k^t_{ijkl} [1 + \cos 3(\varphi_{ijkl} - \varphi^0_{ijkl})], \tag{2}$$

where two atoms i and j define a covalent bond of length r_{ij}; three atoms i, j, and k define bond angle α_{ijk}, and four atoms i, j, k, and l define a dihedral angle φ_{ijkl}. A pair of atoms i and j are considered to be nonbonded if they belong to different molecules or are separated by more than three bonds in the same molecule. The resulting nonbonded interactions (i.e., long-range repulsions and van der Waals interactions) are expressed as

$$V_{\text{nonbonded}} = V_{\text{vdw}} + V_{\text{coulomb}} = \sum_{i<j} [A_{ij} \exp(-B_{ij} r_{ij}) - C_{ij} r^{-6}_{ij}] + \frac{q_i q_j}{r_{ij}}. \tag{3}$$

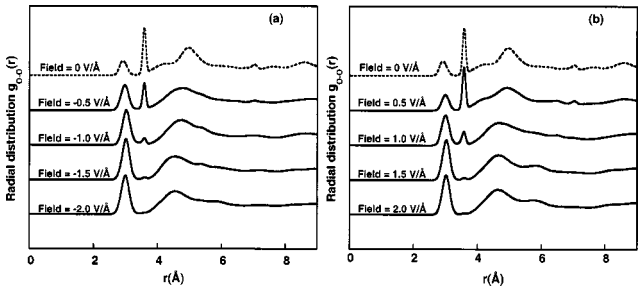

FIG. 1. Effect of electric field on the *gauche* conformation about CC bond in PEG (a) for negative field strengths and (b) for positive field strengths.

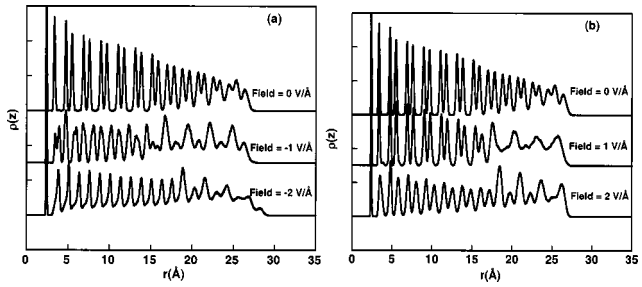

FIG. 3. Calculated density profiles along the surface normal for (a) negative field and (b) positive field are shown.

The van der Waals potential is smoothly truncated at a cutoff radius of $r_c = 9.0$ Å:

$$V_{\mathrm{vdw}}(r) = V_{\mathrm{vdw}}(r) - V_{\mathrm{vdw}}(r_c) - (r - r_c)\frac{dV_{\mathrm{vdw}}}{dr_c}. \tag{4}$$

The Coulomb potential is calculated by the Ewald method. The charges on the PEG atoms are taken from Ref. 12. (The system considered in the Ref. 12 is of the form $H—CH_2—(O—CH_2—CH_2)_m—O—CH_3$, whereas the PEG terminated alkanethiol system has the form $S—(CH_2)_{n-2}H_2C—CH_2—(O—CH_2—CH_2)_m—O—CH_3$. The atoms in bold are assigned the same charge.)

The interactions of sulfur and carbon atoms with gold substrate (i.e., surface interactions) are modeled[13,14] by

$$V_{\mathrm{surface}} = \sum_s \frac{1}{2} k_s^{\mathrm{SF}} d_s^2 + \sum_{pq} \left[\frac{k_{12}^{\mathrm{SF}}}{(z_{pq} - z_p^0)^{12}} - \frac{k_3^{\mathrm{SF}}}{(z_{pq} - z_p^0)^3} \right], \tag{5}$$

where the index s runs over sulfur atoms, p counts the number of chains or molecules, q runs over sulfur and carbon atoms on each molecule, and d_s is the distance of sulfur atom from its original position on the x-y plane. The first term constrains the motion of sulfur atoms on the x-y surface whereas the second term involves the z positions of sulfur and carbon atoms.

The external electric field is modeled by

$$V_{\mathrm{electric}} = q_i E_z z_i, \tag{6}$$

where q_i is the charge of the ith atom, E_z is the electric field strength applied in the z direction, and z_i is the projection of the position vector on the z axis.

The model parameters used in our MD simulations are given in the Refs. 12, 15, and 16.

B. Initial setup and simulation schedule

MD simulations were carried out in NVE ensemble using multiple time step method,[17] with the time step in the inner most loop to be 0.3 fs. The nonbonded computation is done every 3 fs. The PEG terminated SAM system consists of 1500 chains, each with chemical composition of $S—(CH_2)_{13}—(O—CH_2—CH_2)_3—O—CH_3$, on gold surface. To start the simulation, the chains are made in an all-*trans* configuration, tilted initially by about 15° from the normal to the surface, and a temperature of 1 K is given to all the atoms to break the sixfold symmetry. After a thermalization run of 90 ps (300 000 MD steps), the system attained a temperature of ~50 K. The system's temperature is then raised to 200 K in steps of 25 K, over 200 ps. At 200 K, the system has a collective tilt angle of ~34° which is similar to that of methyl-terminated SAMs.[18] It has been shown in previous experiments[19] that the end groups have little effect on the tilt structure of film of *n*-alkyl thiol monolayers on gold. The system is characterized at this temperature and a series of electric fields with varying strengths are applied in the z direction. Henceforth, the field applied parallel and antiparallel to the z axis will be referred to as negative and positive fields, respectively. The strength of the electric fields varies from +2 to −2 V/Å, in steps of 0.5 V/Å. For each value of the electric field, the system is thermalized over 120 ps. If the final temperatures after thermalization run are higher than 200 K, the temperature is decreased to 200 K over a 60 ps

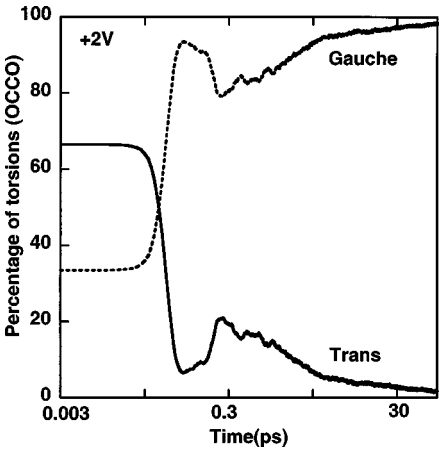

FIG. 2. Time evolution of the *trans* and *gauche* bonds for OCCO torsion with the application of +2 V.

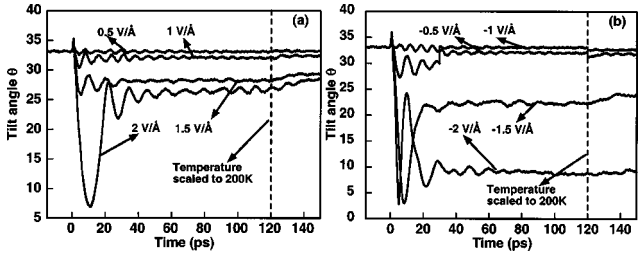

FIG. 4. Effect of electric field on tilt structure for (a) positive field and (b) negative field are shown.

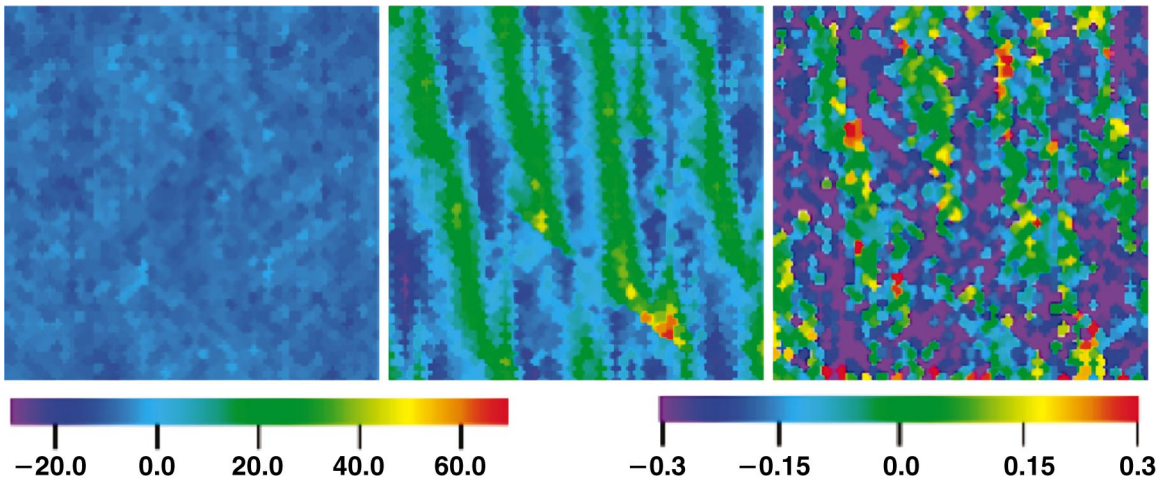

FIG. 5. (Color) 2D structure factors for PEG-terminated SAMs. (a) Field=0, (b) field=2, (c) field=−2 V/Å.

run. To study the reverse transition, the systems with ±2 V/Å electric fields, the field is switched off and the system is thermalized over 90 ps.

III. RESULTS AND DISCUSSION

A. Electric field effect on *gauche* conformations in PEG

We calculate oxygen-oxygen partial radial distribution ($g_{O\text{-}O}$) function in PEG to study the *trans*-to-*gauche* transition in the presence of an applied electric field. In the absence of field, $g_{O\text{-}O}$ has two significant peaks corresponding to *gauche* (~3 Å) and *trans* (~3.8 Å) conformations about C—C bond (O—C—C—O) (see dashed curve in Fig. 1). With no field applied, only the terminal oxygen atom is in *gauche* conformation, with most of the PEG in nearly all-*trans* configuration. Accordingly, the *trans* peak at ~3.8 Å is more pronounced than the *gauche* peak ~3 Å. With the application of electric field, there is a dramatic change in the ratio of *gauche* to *trans* peaks. The intensity of the *gauche* peaks increases while the intensity of the *trans* peaks decreases with the magnitude of the field applied. For the field strengths of ±2 V/Å, the trans peaks almost disappear [see Figs. 1(a) and 1(b)]. The all-*gauche* conformation at high electric fields corresponds to a complete helical structure in PEG. Thus the electric field causes a transition from a mixed *trans*-helical state to a complete helical state.

The power of MD is to be able to predict quantitatively the change in the number of *trans* and *gauche* bonds. In Fig. 2, we show the change in percentage of *gauche* and *trans* bonds with the application of +2 V to OCCO torsion. Before the application of electric field, the percentage of *trans* configuration for the OCCO is 66.5%. With the application of

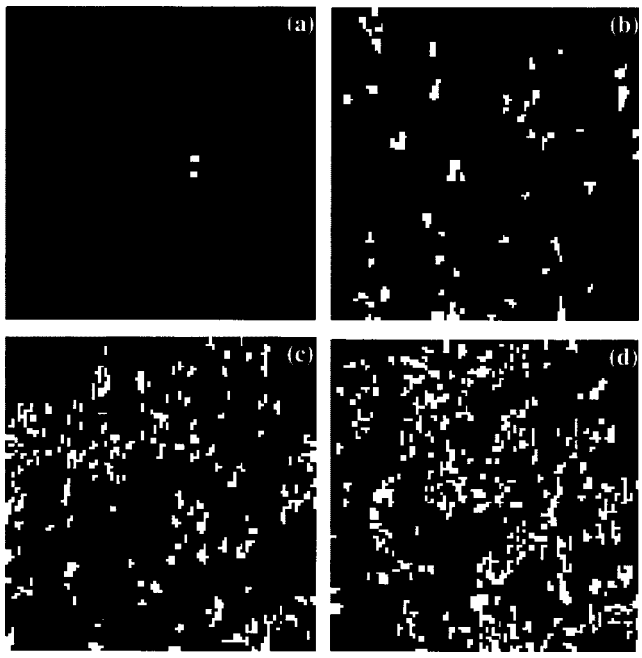

FIG. 6. 2D surface plots of the tilt direction of all the chains in (a) $E_z=0$, (b) $E_z=+2$ V/Å, (c) 2D surface plot of polarity of chains in *Y* direction.

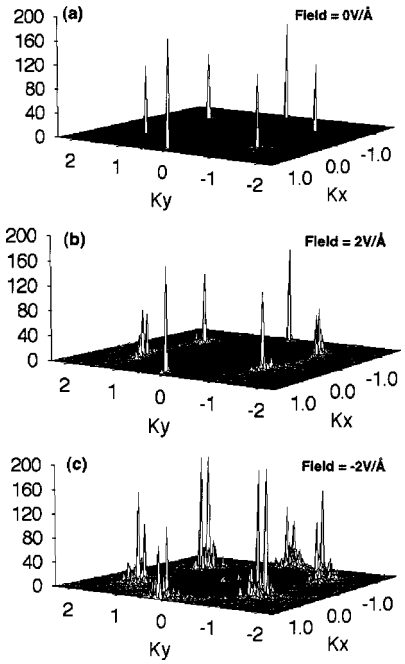

FIG. 7. Surface layer 1 Å below the highest *z* for (a) field=0.5, (b) field=1, (c) field=1.5, (d) field=2 V/Å.

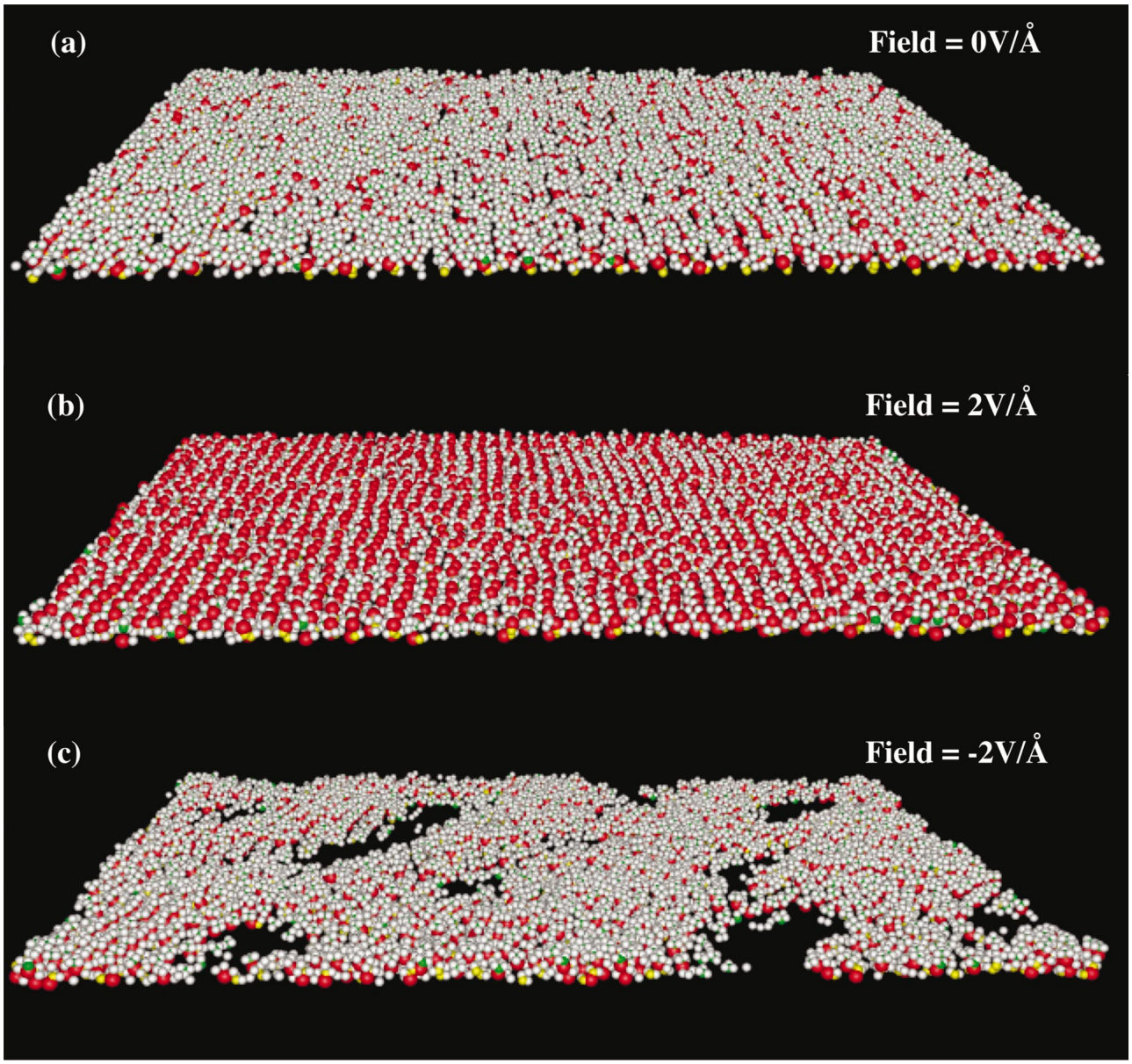

FIG. 8. (Color) The atomic configuration color coded by charges: oxygen (red), hydrogen (white), methyl terminal carbon (yellow) and carbon in PEG (green) in top 6 Å layer of the system. (a) $E_z=0$, (b) $E_z=+2$, (c) $E_z=-2$ V/Å.

electric field, within 30 ps, the *trans* configuration almost disappears and the gauche bonds reach almost 100%, which is also demonstrated in Fig. 1.

We also study the effect of an electric field on the entire chain (both alkanethiol and PEG) using the line density profile of backbone atoms normal to the surface. The calculated profiles at negative and positive fields are shown in Figs. 3(a) and 3(b), respectively. The presence of a doublet pattern in the density plot at $E_z=0$ is an indication of an all-*trans* configuration (the C—C bond takes an alternate sequence of two orientations, nearly parallel and normal, with respect to the surface normal) in the alkanethiol part of the chain. As field strength increases, the doublet pattern becomes less pronounced indicating appearance of *gauche* defects even in the alkanethiol part of the chain. The negative fields affect more adversely the alkanethiol structure than the positive fields, which can be seen by the complete disappearance of doublet pattern in the case of negative electric fields.

B. The effect of electric field on the tilt structure

The tilt structure in SAMs is characterized by two angles, viz., the tilt angle, which is the angle made by the backbone plane of the chain with respect to the surface normal, and the tilt direction, which is the rotation angle about surface normal with respect to the *x* axis. With the electric field, the tilt angle is affected significantly and the deviation from the initial uniform tilt angle increases with the increase in the magnitude of the field strength [see Figs. 4(a) and 4(b)]. The temperature of the system also increases with the application of electric fields because more energy is put into the system. For negative electric fields, the increase in tem-

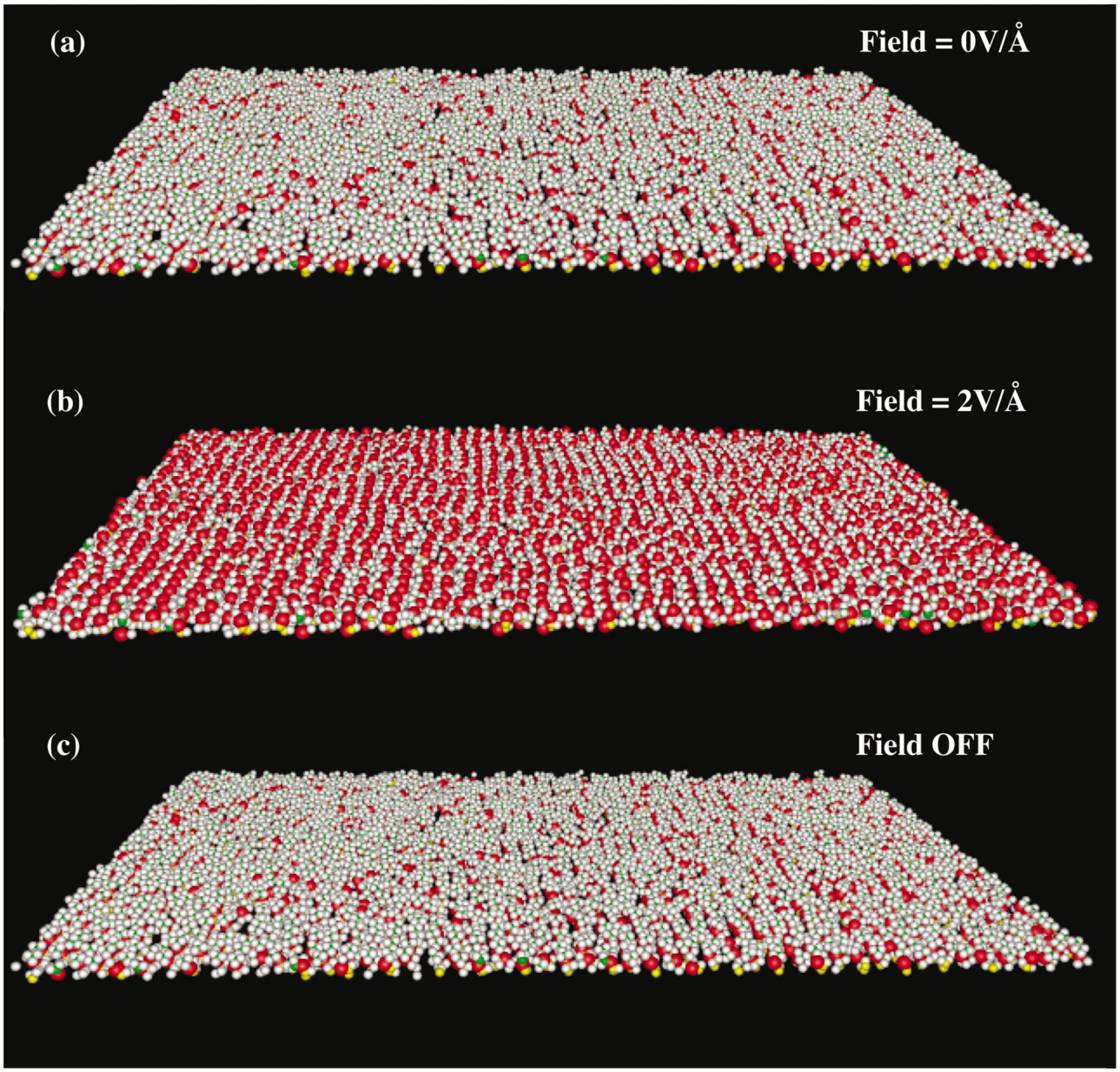

FIG. 9. (Color) The top 6 Å layer of the system (a) before the application of positive electric field, (b) after the application of positive electric field, (c) shows the same layer after the removal of electric field.

perature is higher than for positive fields, because of the increased disorder set in the system with negative fields. The negative field affects the tilt structure more adversely than the positive electric field at high field strengths, which can be seem from Figs. 4(a) and 4(b). In both cases of ± 2 V/Å, the tilt angle initially decreases, but in the case of a negative electric field, the system does not recover from the initial loss of order in the system [see Fig. 4(b)], whereas in the case of a positive electric field, ~75% of the tilt angle is recovered [see Fig. 4(a)]. This is because the negative field tends to pull the oxygen atom towards the substrate, thus introducing disorder in the alkanethiol part of the chain, which destroys the order. The spacing between the chains (~4.8 Å) is not sufficient for the chain to bend completely as was observed in the Ref. 7, where the spacing was ~5.8 Å or greater.

Structural information in the X-Y plane can be probed experimentally using x-ray diffraction[20] and surface x-ray scattering studies.[21] To elucidate the structure of the system under an electric field, we have computed the structure factor $S(k)$,

$$S(k) = \frac{1}{N}\langle |\rho(\mathbf{k})|^2 \rangle, \tag{7}$$

where $\rho(\mathbf{k})$ is the Fourier transform of the local particle density,

$$\rho(\mathbf{k}) = \sum_{i=1}^{N} \exp[-i\mathbf{k}\cdot\mathbf{r}_i] = \sum_{i=1}^{N} \exp[-i(k_x r_{ix} + k_y r_{iy})] \tag{8}$$

and $\mathbf{k}=(k_x,k_y,0)$ represents a two-dimensional scattering vector.

Figure 5 shows the effect of an electric field on the structure factor of the PEG terminated SAMs. Negative electric fields affect the structure factor [see Fig. 5(c)] more than the positive fields [see Fig. 5(b)]. The disorder is also more in the case of negative electric fields and the peak heights are increased because of decrease in the tilt angles of the chains [see Fig. 4(b)].

We also studied the effect of an electric field on the tilt direction of chains. Figures 6(a) and 6(b) show the two-dimensional (2D) surface plots of tilt direction of all the chains. For $E_z=0$, Fig. 6(a) shows the uniform tilt direction distribution $\sim 10°$. For positive polarity, we observed an alternating ''stripe'' pattern in the tilt direction of the system [see Fig. 6(b)]. We find a correlation between the observed pattern in tilt direction and in-plane polarization of the chains. Figure 6(c) shows the polarization of chains in y direction, which has a similar pattern as that of tilt direction plot in Fig. 6(b).

C. Effect of the electric field on the position of the top most oxygen atoms

With the application of a positive electric field more oxygen atoms are exposed near the top of the surface. This can be seen in Fig. 7, which shows the number of exposed oxygen atoms (white) for different strengths of E_z. The thickness of the surface layers shown in Fig. 7 is the top 1 Å. We see very clearly from Fig. 7 that with the increase of the field strength, more and more oxygen atoms come to the top of the layer. This enhanced exposure of oxygen atoms at the surface will increase the hydrophilicity of the surface.

The exposure of oxygen atoms with positive electric field is also seen in Fig. 8, which shows atomic configurations of the top layer of thickness 6 Å of the PEG when $E_z=0$ and ± 2 V/Å, where atoms are color coded by the charge. Hydrogen and oxygen atoms are represented by white and red colors, respectively. Figure 8(a) shows the film with hydrogen atoms (white) exposed and Fig. 8(b) shows the film with positive electric field where the oxygen atoms (red) are exposed. Figure 8(c) shows that with the application of negative electric fields, some chains are depressed leaving behind ''holes'' in the top layer of PEG system [see Fig. 8(c)].

D. Reversible structural transition under an electric field

We also studied whether the electric field induced structural transition is reversible. In Fig. 9, the atomic configuration of top 6 Å layer of the system is shown before the application, after application, and after removal of the positive electric field. The reversible effect can be seen in Fig. 9(c), where after the removal of electric field, the top layers have more hydrogen than oxygen.

The dynamics of the tilt structure during the application and removal of electric fields can be seen in Fig. 10 which shows the tilt angle as a function of time for $E_z=+2$ V/Å [Fig. 10(a)] and $E_z=-2$ V/Å [Fig. 10(b)]. In both the cases

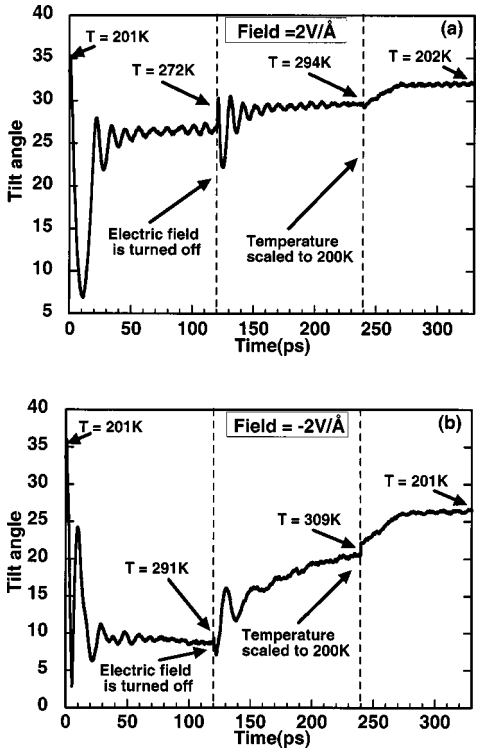

FIG. 10. Plot of the time evolution of tilt angle for (a) $E_z=+2$ and (b) $E_z=-2$ V/Å.

the temperature of the system increased when an electric field is applied as well as when the field is removed.

The increase in temperature, however, is more pronounced in the case of negative fields. We decreased the system temperature after the removal of field to the original temperature in order to compare the systems. It is found that the system to which positive electric field is applied recovers 90% of the tilt angle, whereas the system with negative electric field could recover only 74% of the tilt angle.

The *trans* to *gauche* transition induced by the electric field is reversible with the removal of the electric field, which can be seen in Fig. 11. In Fig. 11, we compare the partial radial distribution of oxygen-oxygen in PEG before and after the application of the electric field at $T=200$ K. The *trans* peak, which completely disappears with the appli-

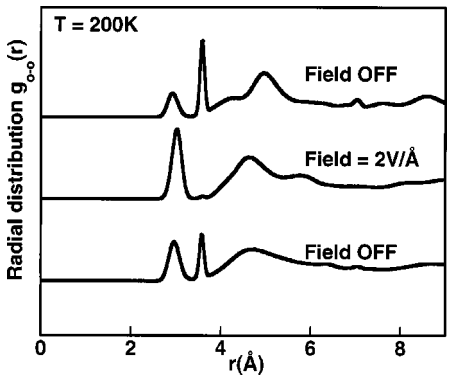

FIG. 11. Reversible transition of *trans-gauche* conformations with and removal of electric field.

cation of the electric field, reappears after the field is removed.

IV. CONCLUSIONS

Molecular dynamics simulations have been performed on parallel computers to study the effect of electric field on the structure of PEG terminated alkanethiol SAM system on gold surface. The electric field triggers a conformational transition from all-*trans* to a mostly *gauche* conformation. The polarity of the electric field has a significant effect on the surface structure of PEG. The electric field applied antiparallel to the surface normal causes a reversible transition to an ordered state where the oxygen atoms are pulled outward. On the other hand, an electric field applied in a direction parallel to the surface normal introduces considerable disorder in the system and the oxygen atoms are pulled inward. The structural difference caused by the polarity of the electric field has a profound effect on the hydrophilicity of the surface. The parallel field affects the overall tilt structure of SAMs more adversely than the antiparallel field.

In a recent work by Lahann *et al.*,[7] the SAMs were synthesized at artificially large lattice constant to facilitate conformational transitions. The terminal group of the SAMs in the experiment is hydrophilic carboxylate (COOH) group having two oxygen atoms, which experience more force in a given electric field (potential applied in the experiment was ~ -1 V). In our simulations, the terminal group has one oxygen atom, and to demonstrate the switching of the surface, we have used artificially high electric fields (-2 to $+2$ V). We are currently performing simulations with carboxylate end groups and at larger lattice constants and expect the transition to occur at much lower electric fields.

ACKNOWLEDGMENTS

This work was supported by AFOSR: DURINT USC-Berkeley-Princeton, AFRL, ARL, NASA, NSF, and Louisiana Board of Regents health excellence fund. Simulations were performed at Department of Defense's Major Shared Resource Centers under CHSSI and Challenge projects, and at LSU's Center for Applied Information Technology and Learning (CAPITAL) and Biological Computation and Visualization Center (BCVC).

[1] *Poly(ethylene glycol) Chemistry: Biotechnical and Biomedical Applications*, edited by J. M. Harris (Plenum, New York, 1992).
[2] S. W. Hui, T. L. Kuhl, Y. Q. Guo, and J. Israelachvili, Colloids Surf., B **14**, 213 (1993).
[3] S. Zalipsky and J. M. Harris, *Poly(ethylene glycol) Chemistry and Biological Applications* (ACS, San Fransisco, CA, 1997), p. 1.
[4] D. Lasic, *Poly(ethylene glycol) Chemistry and Biological Applications* (ACS, San Fransisco, CA, 1997), p. 31.
[5] K. L. Prime and G. M. Whitesides, Science **252**, 1164 (1991).
[6] D. Schwendel, R. Dahint, S. Herrwerth, M. Schloerholz, E. Eck, and M. Grunze, Langmuir **17**, 5717 (2001).
[7] J. Lahann, J. S. Mitragotri, T. Tran *et al.*, Science **299**, 371 (2003).
[8] F. Schreiber, Prog. Surf. Sci. **65**, 151 (2000).
[9] A. J. Pertsin, M. Grunze, and I. A. Garbuzova, J. Phys. Chem. B **102**, 4918 (1998).
[10] M. D. Wilson and G. M. Whitesides, J. Am. Chem. Soc. **110**, 8718 (1988).
[11] P. Harder, M. Grunze, R. Dahint, G. M. Whitesides, and P. E. Laibinis, J. Phys. Chem. B **102**, 426 (1998).
[12] G. D. Smith, R. L. Jaffe, and D. Y. Yoon, J. Phys. Chem. **97**, 12752 (1993).
[13] J. Hautman and M. L. Klein, J. Chem. Phys. **91**, 4994 (1989).
[14] J. P. Bareman and M. L. Klein, J. Phys. Chem. **94**, 5200 (1990).
[15] A. J. Pertsin and M. Grunze, Langmuir **10**, 3668 (1994).
[16] R. A. Sorensen, W. B. Liau, L. Kesner, and R. H. Boyd, Macromolecules **21**, 200 (1988).
[17] M. Tuckerman, B. J. Berne, and G. J. Martyna, J. Chem. Phys. **97**, 1990 (1992).
[18] S. Vemparala, B. B. Karki, R. K. Kalia, A. Nakano, and P. Vashishta, J. Chem. Phys. (to be published).
[19] R. G. Nuzzo, L. H. Dubois, and D. L. Allara, J. Am. Chem. Soc. **112**, 558 (1990).
[20] K. Kjaer, J. Als-Nielsen, C. A. Helm, L. A. Laxhuber, and H. Mohwald, Phys. Rev. Lett. **58**, 2224 (1987).
[21] P. Dutta, J. B. Peng, B. Lin, J. B. Ketterson, M. Prakash, P. Georgopoulos, and S. Ehrlich, Phys. Rev. Lett. **58**, 2228 (1987).